To appear in Proceedings of the 29th Intern. Conf. on Coastal Eng. 2004

A THIRD-GENERATION SPECTRAL WAVE MODEL USING AN UNSTRUCTURED FINITE VOLUME TECHNIQUE

OLE R. SØRENSEN, HENRIK KOFOED-HANSEN,
MORTEN RUGBJERG, LARS S. SØRENSEN

DHI Water & Environment, Agern Allé 5, DK-2970 Hørsholm, Denmark

A new third-generation spectral wave model is presented for prediction of the wave climates in offshore and coastal areas. The essential topic of the present paper is new numerical techniques for solution of the governing equations. The discretisation in the geographical space and the spectral space is based on cell-centred finite volume technique. In the geographical space, an unstructured mesh is applied. Due to the high degree of flexibility, unstructured meshes are very efficient to deal with problems of different characteristic scales. The time integration is performed using a fractional step approach, where an efficient multisequence explicit method is applied for the propagation process. The model is verified by comparison with observations for two real field cases.

1. Introduction

Third-generation wave models are used extensively for prediction of the growth, decay and transformation of wind-generated waves and swell in the deep ocean and shelf seas. Recently, these models have been extended for application in coastal areas. The main focus has so far been on the formulation of the source functions describing the different physical phenomena, which are important in shallow water. The essential topic of the present paper is new numerical techniques for solution of the governing equations.

Traditionally, third-generation spectral wave models are solved using either an Eulerian or a semi-Lagrangian approach on rectangular structured meshes. Even with the computers of today, these models are very computational demanding. To resolve the characteristic scales of the important physical phenomena in the coastal areas, a fine mesh is required. In the breaking zone, a resolution of the order of 10m is needed. A high resolution is also needed to resolve the complex bottom topographies in shallow water environments, such as barrier islands, reefs, submerged bars, and channels. The need for high-resolution local models can be achieved by using the nesting technique, where a local model with a fine mesh is embedded in a coarse mesh model. Usually, only a one-way transfer of boundary condition from the coarse mesh model to the fine mesh model is used. With the goal of reducing the computational effort, it is desirable to introduce more flexible meshes as an alternative to nested models. Control of node distribution allows for optimal usage of nodes and adaption of mesh resolution to the relevant physical scales. Flexible meshes can be accomplished in a number of ways, e.g. multi-block curvilinear meshes, overlapping meshes, local mesh refinement and unstructured meshes. Only a few examples of third-

generation spectral model using flexible meshes have been presented. Recently, the possibility of using curvilinear meshes has been implemented in the SWAN model (Booij et al., 1999), however, so far only in a single-block mode. Benoit el al. (1996) developed the model TOMAWAC based on semi-Lagrangian approach, where an unstructured finite element technique was used for the spatial discretisation of the dependent variables.

In this paper, a new Eulerian model based on unstructured meshes is developed. The unstructured mesh approach has been chosen because it gives the maximum degree of flexibility. In coastal regions, the effect of tides, surges and currents can be very important for accurate prediction of the wave conditions. In the presence of dynamic depths and currents, the conserved quantity is wave action and the dynamics of the gravity waves can be described by the conservation equation for wave action density. For small-scale applications, the basic conservation equations are usually formulated in Cartesian co-ordinates, while spherical polar co-ordinates are used for large-scale applications. The source functions implemented in the new model are based on state-of-the-art third-generation formulations.

The spatial discretisation of the conservation equation for wave action is performed using an unstructured finite volume (FV) method. During the last decade, FV methods have been successfully applied for modelling of non-linear transport problems and compressible flow problems. The time integration is based on a fractional step approach, where the propagation step is solved using an explicit method. The use of explicit method can introduce a severe restriction on the time step for a given spatial discretisation due to the CFL stability condition. In order to relax the restriction on the time step, a multisequence explicit integration scheme is applied.

2. Governing Equations

In the present model, the wind waves are represented by the action density spectrum $N(\sigma,\theta)$. The independent phase parameters have been chosen as the relative (intrinsic) angular frequency, $\sigma = 2\pi f$, and the direction of wave propagation, θ. The governing equation is the wave action balance equation formulated in either Cartesian or spherical co-ordinates (see Komen et al., 1994 and Young, 1999). In horizontal Cartesian co-ordinates, the conservation equation for wave action can be written as

$$\frac{\partial N}{\partial t} + \nabla \cdot (\bar{v} N) = \frac{\left(S_{in} + S_{nl} + S_{ds} + S_{bot} + S_{surf}\right)}{\sigma} \qquad (1)$$

where $N(\bar{x},\sigma,\theta,t)$ is the action density, t is the time, $\bar{x} = (x, y)$ is the Cartesian co-ordinates, $\bar{v} = (c_x, c_y, c_\sigma, c_\theta)$ is the propagation velocity of a wave group in

the four-dimensional phase space $\vec{x}$, σ and θ. ∇ is the four-dimensional differential operator in the $\vec{x}$, σ, θ-space.

The source functions on the right side of Eq (1) represent various physical phenomena. The wind input, S_{in}, is based on Janssens's quasi-linear theory of wind-wave generation (Janssen, 1989, 1991), and implemented as in WAM Cycle 4 (see Komen et al., 1994). The non-linear energy transfer, S_{nl},, through the four-wave interaction is represented by the discrete interaction approximation (DIA) proposed by Hasselmann et al. (1985). The source function describing the dissipation due to whitecapping, S_{ds}, is based on the theory of Hasselmann (1974), tuned according to Janssen (1989) and Janssen and Günter (1992). The rate of dissipation, S_{bot}, due to bottom friction is based on linear theory (see Weber, 1991 and Johnson and Kofoed-Hansen, 2000). The friction coefficient is determined as the product of a friction factor and the rms orbital velocity at the bottom. The friction factor is calculated using the expression by Jonsson (1966) and Jonsson and Carlson (1976). In the expression by Jonsson, the friction coefficient is determined as function of the bottom roughness length scale, k_N, and the orbital displacement at the bottom. Depth-induced breaking occurs when waves propagate into very shallow areas, and the wave height can no longer be supported by the water depth. The formulation of the source term, S_{surf} , due to wave breaking is based on the breaking model by Battjes and Janssen (1978). Eldeberky and Battjes (1995) proposed a spectral formulation of this breaking model, where the spectral shape was not influenced by breaking.

3. Numerical Method

3.1. Space Discretisation

The discretisation in geographical and spectral space is performed using a cell-centred finite volume method. In the geographical domain, an unstructured mesh is used. The spatial domain is discretised by subdivision of the continuum into non-overlapping elements. The elements can be of arbitrarily shaped polygons, however, in this paper only triangles are considered. The action density, $N(\vec{x}, \sigma, \theta)$ is represented as a piecewise constant over the elements and stored at the geometric centres. In frequency space, a logarithmic discretisation is used

$$\sigma_1 = \sigma_{\min} \qquad \sigma_l = f_\sigma \sigma_{l-1} \qquad \Delta\sigma_l = \sigma_{l+1} - \sigma_{l-1} \qquad l = 2, N_\sigma$$

where f_σ is a given factor, σ_{min} is the minimum discrete angular frequency and N_σ is the number of discrete frequencies. In the directional space, an equidistant discretisation is used

$$\theta_m = (m-1)\Delta\theta \qquad \Delta\theta_m = 2\pi / N_\theta \qquad m = 1, N_\theta$$

where N_θ is the number of discrete directions. The action density is represented as piecewise constant over the discrete intervals, $\Delta\sigma_l$ and $\Delta\theta_m$, in the frequency and directional space.

Integrating Eq (1) over area A_i of the ith element, the frequency increment $\Delta\sigma_l$ and the directional increment $\Delta\theta_m$ give

$$\frac{\partial}{\partial t}\int_{\Delta\theta_m}\int_{\Delta\sigma_l}\int_{A_i} N d\Omega d\sigma d\theta - \int_{\Delta\theta_m}\int_{\Delta\sigma_l}\int_{A_i}\frac{S}{\sigma} d\Omega d\sigma d\theta = \int_{\Delta\theta_m}\int_{\Delta\sigma_l}\int_{A_i}\nabla\cdot(\overline{F}) d\Omega d\sigma d\theta \tag{2}$$

where Ω is an integration variable defined on A_i and $\overline{F} = (F_x, F_y, F_\sigma, F_\theta) = \overline{v}N$ is the convective flux. The volume integrals on the left-hand side of Eq (2) are approximated by one-point quadrature rule. Using the divergence theorem, the volume integral on the right-hand can be replaced by integral over the boundary of the volume in the $\overline{x}$, σ, θ-space and these integrals are evaluated using a midt-point quadrature rule. Hence, Eq (2) can be written

$$\frac{\partial N_{i,l,m}}{\partial t} = -\frac{1}{A_i}\left[\sum_{p=1}^{NE}(F_n)_{p,l,m}\Delta l_p\right] - \frac{1}{\Delta\sigma_l}\left[(F_\sigma)_{i,l+1/2,m} - (F_\sigma)_{i,l-1/2,m}\right] - \frac{1}{\Delta\theta_m}\left[(F_\theta)_{i,l,m+1/2} - (F_\theta)_{i,l,m-1/2}\right] + \frac{S_{i,l,m}}{\sigma_l} \tag{3}$$

where NE is the total number of edges in the cell (NE = 3 for triangles). $(F_n)_{p,l,m} = \left(F_x n_x + F_y n_y\right)_{p,l,m}$ is the normal flux through the edge p in the geographical space with length Δl_p. $\overline{n} = (n_x, n_y)$ is the outward pointing unit normal vector of the boundary in the geographical space. $(F_\sigma)_{i,l+1/2,m}$ and $(F_\theta)_{i,l,m+1/2}$ are the flux through the face in the frequency and directional space, respectively.

The convective flux is derived using a first-order upwinding scheme. The numerical diffusion introduced using first-order upwinding schemes can be significant for the case of swell propagation over long distances, see e.g. Tolman (1991, 1992). In small-scale coastal applications and application dominated by local wind, the accuracy obtained using these schemes is considered to be sufficient.

3.2. Time Integration

The integration in time is based on a fractional step approach. Firstly, a propagation step is performed calculating an approximate solution at the new time level by solving Eq (2) without the source terms. Secondly, a source term step is performed calculating the new solution from the estimated solution taking into account only the effect of the source terms.

The propagation step is carried out by an explicit Euler scheme. To overcome the severe stability restriction, a multisequence integration scheme is employed following the idea by Vislmeier and Hänel (1995). Here, the maximum time step is increased by locally employing a sequence of integration steps, where the number of steps may vary from element to element. Using the explicit Euler scheme, the time step is limited by the CFL condition stated as

$$Cr_{i,l,m} = \left| c_x \frac{\Delta t}{\Delta x_i} \right| + \left| c_y \frac{\Delta t}{\Delta y_i} \right| + \left| c_\sigma \frac{\Delta t}{\Delta \sigma_l} \right| + \left| c_\theta \frac{\Delta t}{\Delta \theta_m} \right| < 1 \qquad (4)$$

where $Cr_{j,l,m}$ is the Courant number and Δx_i and Δy_i are characteristic length scale in the x and y-directions for the ith element. The maximum local Courant number, $Cr_{max,\,i}$, is determined for each element in the geographical space, and the maximum local time step is given by $\Delta t_{\max,i} = \Delta t / Cr_{\max,i}$. To ensure accuracy in time, the intermediate levels have to be synchronised. The time step index g is determined as the minimum value for which

$$\Delta t\, f_g < \Delta t_{\max,i} \qquad f_g = \left(\frac{1}{2}\right)^{g-1}, \qquad g = 1, 2, 3, \ldots \qquad (5)$$

The local time step is then determined as $\Delta t_{\,i} = \Delta t\, f_g$. Two neighbouring elements are not allowed to have an index difference greater than one.

The calculation is performed using a group concept, in that groups of elements are identified by their index, *g*. The computational speed-up using the multisequence integration compared to the standard Euler method increases with increasing number of groups. However, to get accurate results in time, the maximum number of groups must be limited. In the present work, the maximum number of levels is 32.

4. Numerical Experiments

In order to verify the accuracy of the numerical approach, a large number of test cases have been conducted. These include simple tests of both depth-induced and current-induced shoaling and refraction of monochromatic, long-crested waves for which analytical solutions can be obtained. The agreement with the analytical solutions was excellent. In the present paper, we will focus on two real

applications where measurements are available.

4.1. Storm of 29 January 2002 in the North Sea

The storm of 29 January 2002 was severe. The storm was caused by a depression travelling from England towards the eastern part of the North Sea. The storm produced prolonged strong westerly winds with a maximum 10m wind speed of approximately 26m/s. The simulation period chosen for the numerical simulations runs from 00 UTC 22 January 2002 to 00 UTC 31 January 2002.

The computational domain covers part of the Norwegian Sea, the North Sea, the Inner Danish Waters, the Baltic Sea and the Gulf of Botnia. Special emphasis is devoted the prediction of the wave conditions at Horns Rev (reef) in the south eastern part of the North Sea. At this site, a 168 MW offshore wind farm with 80 turbines have been established. The numerical model has been used to forecast the wave conditions during the construction in 2002, and is subsequently being used in connection with maintenance. An unstructured mesh containing 8985 triangular elements is used: in the Norwegian Sea the element size is approximatively 800km^2, in the North Sea, the Baltic Sea, and the Gulf of Botnia the element size is approximatively 200km^2, in the inner Danish Waters the element size is approximatively 50km^2 and finally in the Horns Rev area a very fine mesh with an element size of 1.5km^2 is applied. The mesh is shown in Figure 1 and a close-up of the mesh in the area at Horns Rev is shown in Figure 2. A fine mesh is required in the area at Horns Rev due to the complex topography characterised by a system of reefs (see Figure 2). A logarithmic frequency discretisation with 25 frequencies is used. The lowest discrete frequency is f_{min} = 0.04Hz and the ratio between successive frequencies is chosen as f_σ = 1.115. The number of discrete directions is chosen as 16. The overall time step in the simulation is 600s. The averaged number of levels in the propagation step is 6. Hence, a speed-up of a factor 6 for the propagation is obtained using the multisequence integration scheme compared to using a standard Euler scheme.

The wind data for the storm of January 2002 have been provided from Vejr2's meteorological ETA model (www.vejr2.dk). The data consist of 10m wind speed and the wind direction every three hours. At Horns Rev, the tidal range is approximatively 1.5m and during a storm the setup due to storm surge can be up to 2.5m. The minimum water depth at Horns Rev is 3-4m. Hence, to get accurate prediction of the wave conditions during a storm, it is important to include the effect of tidal variation and storm surge. Therefore, the time-varying water depth is included in the wave simulation. The time-varying water depths are calculated using a two-dimensional hydrodynamic model (MIKE 21 Flow Model FM). For the parameter in the breaking formulation, γ = 0.8 is applied and for the bed friction, a Nikuradse roughness k_N = 0.04m is applied.

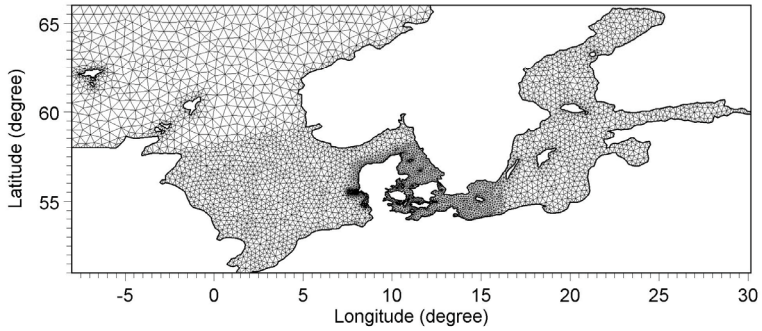

Figure 1. The computational mesh.

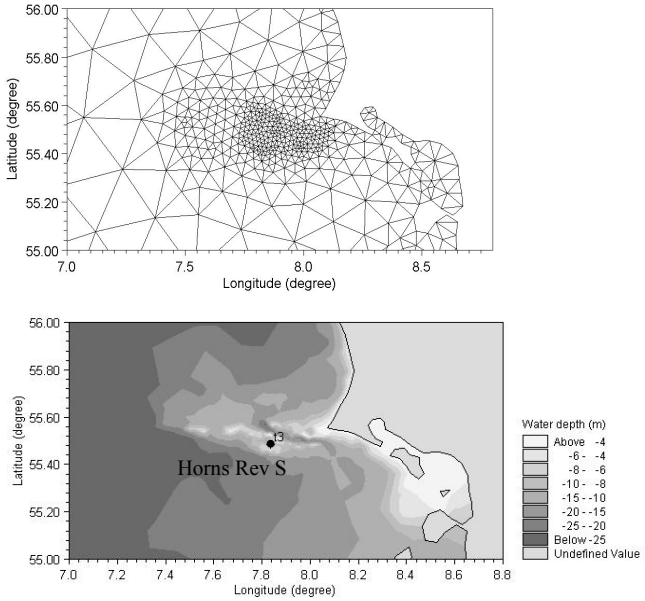

Figure 2. Close-up of the computational mesh (a) and of the bathymetry (b) at Horns Rev. The location of the buoy is shown on the plot (t3).

The results from the numerical model are compared to observations at two locations: Fjaltring ((ϕ,λ)=(8.0582°E, 56.4750°N) and depth 17.5m) and Horns Rev S ((ϕ,λ)=(7.8367°E, 55.4836°N) and depth 10.0m). The measurements are obtained using a Datawell Waverider Buoy. At Horns Rev S, the buoy is located on the south side of the shallow submerged reef (see Figure 2) and the wave condition is strongly influenced by wave breaking on the reef for waves coming from westerly to northerly directions.

Time series of calculated and measured integral wave parameters are compared in Figures 3 and 4, respectively at Fjaltring and Horns Rev S. The

integral parameters are the significant wave height, H_{m0}, the mean period, T_{02}, and the peak period, T_p. The agreement between the numerical results and the observations is generally very good. To test the effect of including the time-varying water depth due to tide and surge, a simulation was also performed without this effect. As expected, the effect was very small at Fjaltring because the water depth of 17.5m is large compared to the variation in the water level. However, at Horns Rev S, the effect was very significant. When the time-variation of the depth is excluded, the significant wave height is significantly underestimated at the peak of the storm.

4.2. Gellen Bay

The second case is to simulate the time evolution of wave conditions in a micro-tidal environment in a bay of the German Baltic coast during a significant storm event that resulted in intense wave activity. During the simulation period of nine days in January 2000, the water level varied in the range from -0.5 to 1.0m due

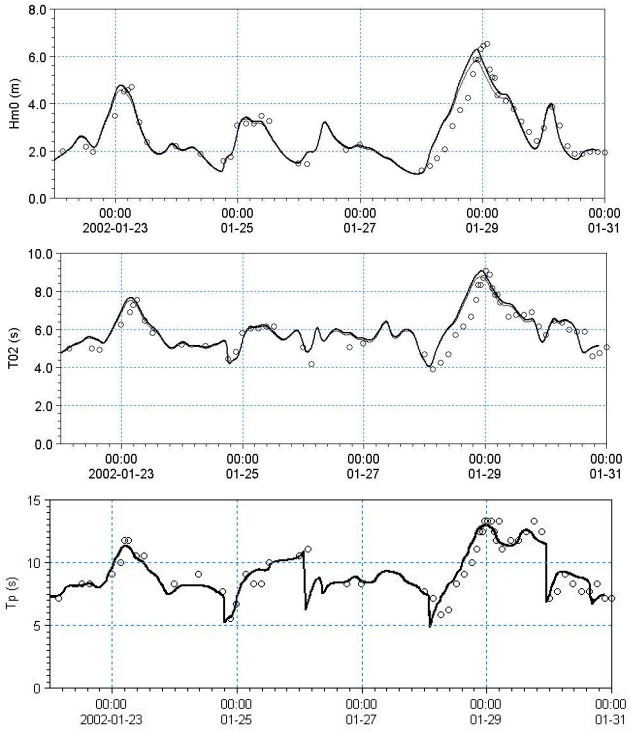

Figure 3. Time series of significant wave height, H_{m0}, mean wave period, T_{02}, and peak wave period, T_P, at Fjaltring. —— Calculations (including time-varying depth), — calculations (excluding time-varying depth) and o measurements.

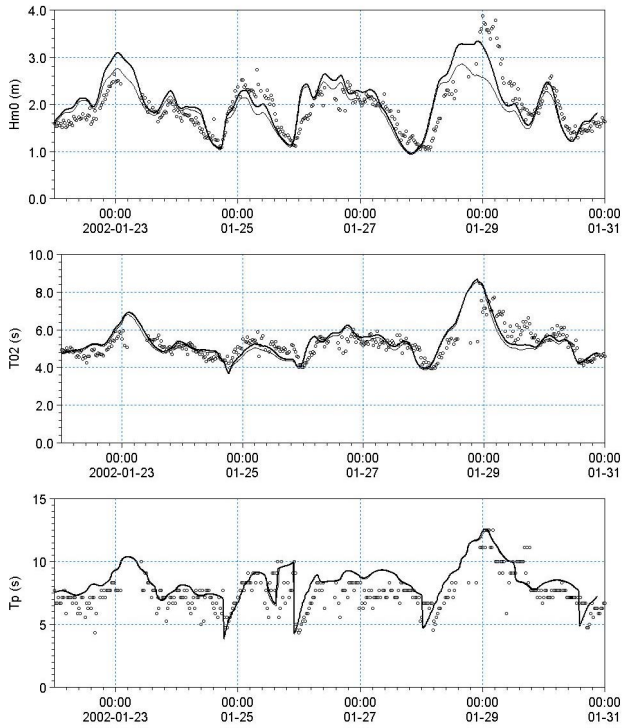

Figure 4. Time series of significant wave height, H_{m0}, mean wave period, T_{02}, and peak wave period, T_p, at Horns Rev S. ▬▬ Calculations (including time-varying depth), ── calculations (excluding time-varying depth) and o measurements.

to tidal variations and storm surge. Hence, to get accurate prediction of the wave conditions in the nearshore areas time-varying water depth is included in the wave simulation. The main area, of interest is the shoreline of the island Hiddensee and the coast of the Zingst peninsula. The Gellen Bay area was studied extensively within the MORWIN project (Lehfeldt and Barthel, 1999, and Lehfeldt et al., 2002).

The mesh contains 9420 elements. The maximum edge length is approximately 6.5km and the minimum edge length is 400m near the shoreline in the main area of interest. The mesh is shown in Figures 5 and 6. A logarithmic frequency discretisation with 25 frequencies is used. The lowest discrete frequency is f_{min} = 0.055Hz and the ratio between successive frequencies is chosen as f_σ = 1.1. The number of discrete directions is chosen as 18. The overall time step is 150s. The averaged number of levels in the propagation step is 4.5.

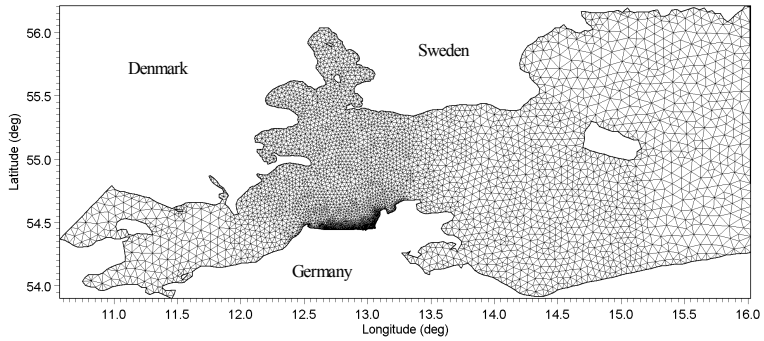

Figure 5. The computational mesh

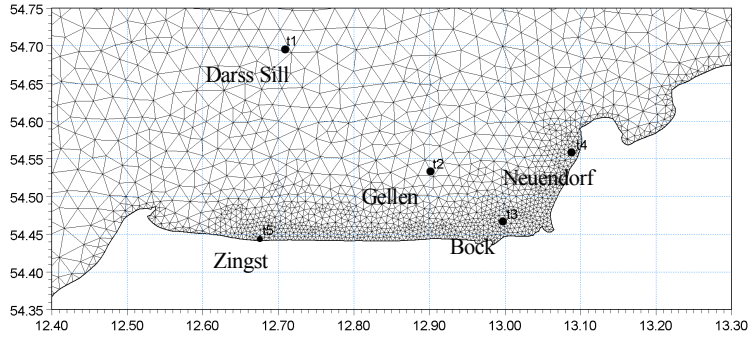

Figure 6. Close-up of the computational mesh.

The wave conditions offshore at Darss Sill (t1: 20.5m depth) and at a nearshore station close to Zingst (t2: 4.5m depth) have been measured continuously for several years. As part of the MORWIN project measurements of the wave conditions at three additional locations were performed: Gellen (t3: 8.3m depth), Bock (t4: 5.5m depth) and Neuendorf (t5: 6.5m depth). The locations are shown in Figure 6.

Time series of calculated and measured integral wave parameters are compared in Figures 7 through 9. It can be seen that the wave conditions are well reproduced both offshore and in more shallow water near the shore. Table 1 shows the wave statistic at the five stations based on the observed and calculated significant wave height. The mean error (Bias), r.m.s. error (RMS), bias index (BI), scatter index (SI) and correlation coefficient (CC) are listed for each station. The bias index and scatter index are obtained by normalizing the mean error and the r.m.s. error, respectively, with the observed mean value. The RMS values are less than 0.25m at all stations. At Zingst and Neuendorf, the scatter index is somewhat higher than at the three other stations due to the small mean values. The correlation between observations and calculations is high.

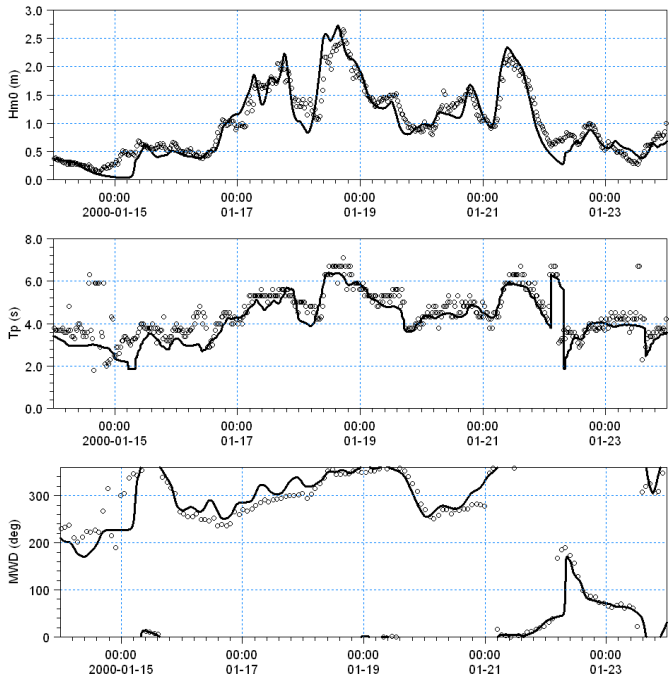

Figure 7. Time series of significant wave height, H_{m0}, peak wave period, T_p , and mean wave direction, MWD, at Darss sill (Offshore). ▬ Calculation and o measurements.

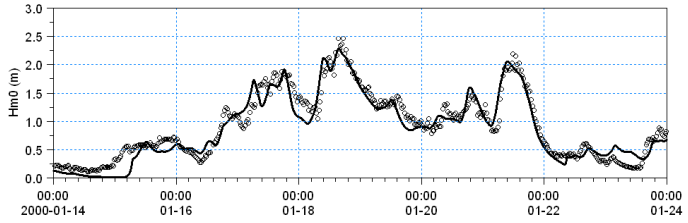

Figure 8. Time series of significant wave height, H_{m0}, at Gellen. ▬ Calculation and o measurements.

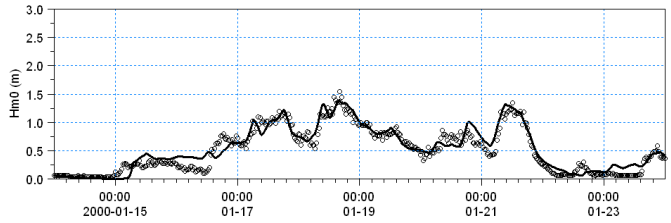

Figure 9. Time series of significant wave height, H_{m0}, at Bock. ▬ Calculation and o measurements.

Table 1. Statistical parameter at the five stations (see Figure 6).

Station	Bias (m)	RMS (m)	BI	SI	CC
Darss Sill, t1	0.037	0.206	-0.037	0.208	0.949
Gellen, t2	0.048	0.177	-0.054	0.201	0.957
Bock, t3	0.031	0.121	0.065	0.252	0.953
Zingst, t4	0.085	0.194	0.175	0.401	0.931
Neuendorf, t5	0.156	0.225	0.310	0.446	0.956

5. Conclusion

A new third-generation spectral model is presented. The model is based on the finite volume method, where an unstructured mesh is applied in the geographical domain. The time integration is performed using an efficient multisequence explicit scheme. The new numerical spectral model is part of DHI's MIKE 21 SW wave model. To verify the performance and accuracy of the new model, results have been compared with observations for two real applications. The agreement between the model results and measurements is found to be excellent.

The new numerical approach enables the accurate computations of the wave conditions in offshore and coastal areas including the effect of time-varying depths and currents. Due to the high degree of flexibility, unstructured meshes are very efficient to deal with problems of different characteristic scales. In coastal areas, a fine grid is needed to resolve the important physical phenomena and resolve complex bottom topographies, while in offshore areas coarser resolution is usually sufficient.

Acknowledgements

This research was partly funded by Eltra (the Electricity Transmission Company for Jylland and Fyn) as part of its "Public Service Obligation" (PSO), Project No 3187 - "Bølgeprognosemodeller". Their financial support is greatly appreciated. The observations at Horns Rev S were supplied by Elsam A/S and at Fjaltring by Kystdirektoratet. The observations for the Gellen Bay case were supplied by the MORWIN project.

References

Battjes, J.A. and J.P.F.M. Janssen, (1978), Energy loss and set-up due to breaking of random waves, *Proc. 16th Int. Conf. Coastal Eng.,* ASCE, 569-587.

Benoit, M., F. Marcos and F. Becq, (1996), Development of a third-generation shallow water wave model with unstructured spatial meshing, *Proc. 25th Int. Conf. Coastal Eng*., ASCE, 465-478.

Booij, N., R. C. Ris and L. H. Holthuijsen, (1999), A third-generation wave model for coastal regions. 1. Model description and validation. *J. Geophys. Res*., **104**, 7649-7666.

Eldeberky, Y. and J.A. Battjes. (1995), Parameterization of triad interactions in wave energy models, paper presented at Coastal Dynamics Conference, ASCE., Gdansk, Poland.

Hasselmann K., (1974), On the spectral dissipation of ocean waves due to whitecapping, *Bound. Layer Meteor.*, **6**, 107-127.

Hasselmann, S., K. Hasselmann, J.H. Allender and T.P. Barnett, (1985), Computations and parameterizations of the non-linear energy transfer in gravity wave spectrum. Part II: Parameterisations of non-linear energy transfer for applications in wave models, *J. Phys. Oceanog.*, **15**, 1369-1377.

Komen, G.J, L. Cavaleri, M. Doneland, K. Hasselmann, S. Hasselmann and P.A.E.M. Janssen, (1994), *Dynamics and modelling of ocean waves*, Cambridge University Press, UK, 560 pp.

Lehfeldt R. and Barthel V., (1999), MORWIN – Collaborative Modeling of Coastal Morphodynamics, in Spauding ML, Butler HL (eds), Proc. 6th Int. Conf. Estuarine and Coastal Modeling, 1192-1205.

Lehfeldt R., Milbrandt P., Zyserman J.A. and Barthel V., (2002), Evaluation of simulation models used for morphodynamic studies, *Proc. 28th Int. Conf. Coastal Eng.*, ASCE, 3357-3359.

Janssen, P.A.E.M., (1989), Wave-induced stress and the drag of airflow over sea waves, *J. Phys. Oceanogr.*, **19**, 745-754.

Janssen, P.A.E.M., (1991), Quasi-linear theory of wind-wave generation applied to wave forecasting, *J. Phys. Oceanogr.*, **21**, 1631-1642.

Janssen P.A.E.M. and Günther, (1992), Consequences of the effect of surface gravity waves on the mean air flow, *Int. Union of Theor. and Appl. Mech. (IUTAM)*, Sydney, Australia, 193-198.

Johnson H.K., and H. Kofoed-Hansen, (2000), Influence of bottom friction on sea roughness and its impact on shallow water wind-wave modelling, *J. Phys. Oceanogr.*, **30**, 1743-1756 .

Jonsson, I.G., (1966), Wave boundary layers and friction factors, *Proc. 10th Int. Conf. Coastal Eng.,* Tokyo, ASCE, 127-148.

Jonsson I.G. and N.A. Carlsen, (1976), Experimental and theoretical investigations in an oscillatory turbulent boundary layer, *J. Hydraul. Res.*, **14**, 45-60.

Tolman, H.L., (1991), A third generation model for wind waves on slowly varying, unsteady and inhomogeneous depths and currents, *J. Phys. Oceanogr.*, **21**, 782-797.

Tolmann, H.L. (1992), Effects of numerics on the physics in a third-generation wind-wave model, *J. Phys. Oceanogr*, **22**, 1095-1111.

Vilsmeier R. and D. Hänel, (1995), Adaptive solutions for unsteady laminar flows on unstructured grids, *Int. J. Numer. Meth. Fluids*, **22**, 85-101.

Young I.R., (1999), Wind-generated ocean waves, In Elsevier Ocean Engineering Book Series, Volume 2. Eds. R. Bhattacharyya and M.E. McCormick, Elsevier.

Weber, S.L, (1991), Bottom friction for wind sea and swell in extreme depth-limited situations, *J. Phys. Oceanogr.*, **10**, 1712-1733.